

Roles of an inward particle flux inducing quasi-coherent mode in pedestal dynamics and ELM onset in H-mode plasmas

J.Q.Dong^{1,2}, J.Cheng¹, K.Itoh³, L.W.Yan¹, Z.H.Huang¹, Y.Shen¹, H.D. He¹, J.Q.Xu¹, M. Jiang¹, X.Q.Ji¹, K.J.Zhao¹, W.L.Zhong¹, Y.G.Li¹, D.L.Yu¹, S.-I. Itoh⁴, S. Inagaki⁴, Z.B.Shi¹, X. L.Zou⁵, Q.W.Yang¹, X.T. Ding¹, X.R. Duan¹

¹Southwestern Institute of Physics, P. O. Box 432, Chengdu, Sichuan 610041, China

²Institute for Fusion Theory and Simulation, Zhejiang University, 310027, China

³National Institute for Fusion Science, Oroshi-cho, Toki 509-5292, Japan

⁴Research Institute for Applied mechanics, Kyushu University, 816-8580, Japan

⁵CEA, IRFM, F-13108 Saint-Paul-lez-Durance, France

E-mail contact of main author:jiaqi@swip.ac.cn

Abstract. Detailed analyses of the dynamic evolutions of plasma parameters, including density, temperature, pressure and their gradients in pedestal were performed in recent H-mode experiments on HL-2A tokamak. Dramatic increase of density gradient, and slight decrease of electron temperature gradient were observed in the pedestal just prior to each ELM onset in a series. An inward particle flux inducing quasi-coherent mode (QCM) was found to be responsible for such changes, and inducing the ELM onset. The mode was observed in floating potential, density and its gradient, radial electric field etc. and grows very rapidly just about 200 microseconds before each ELM onset. The auto-power spectrum analysis indicates that the mode frequency peaks at $f \sim 40\text{-}60$ kHz. The characteristics of the mode are identified. The squared auto-bicoherence analyses of the floating potential and density fluctuations indicate that the mode has strong nonlinear interaction with the ambient turbulence. The mode induced inward particle flux plays a dominant role in the particle balance and increases of density and its gradient in the pedestal before each ELM onset. The mode also induces increases of plasma pressure and its gradient and may play a key role in triggering of ELM onset. The role of mode induced energy transport is small in the energy balance, indicating decoupling of particle diffusion from energy transport, similar to that observed in I-mode discharges. In addition, the gradient scale length of electron density is always shorter than that of temperature at the starting point of the ELM onset and, therefore, the dominant role of density gradient over temperature gradient for ELM inducing is demonstrated. The results are consistent with I-mode discharges where high temperature gradient does not lead to ELM and in contrast with the previously reported quasi-coherent modes which play significant roles in sustaining H-mode discharges

1. Introduction

In an L-H transition process, a transport barrier usually develops in a narrow region, called pedestal, at plasma edge [1]. The accumulation of energy and particles inside the pedestal normally leads to explosive relaxation of plasma pressure gradients in the pedestal via edge localized modes (ELMs) which are understood as MHD peeling/ballooning instability [2]. The behaviors of pedestal pressure gradient collapse and rebuild during and after each ELM eruption have significant influence not only on plasma performance but also on safety of in-vessel components such as first wall and divertor [3-4]. Therefore, the dynamic evolutions of plasma parameters, including density, temperature, pressure and their gradients in pedestal in inter-ELM phases, and induction of ELMs in particular is under intensive investigation.

Despite growing efforts in pedestal transport modeling, there is no consensus to date on mechanism for the residual electron heat transport in the pedestal. As far as particle transport is concerned, a strong particle pinch (inward flux) may offset strong particle diffusion in the edge pedestal. However, no direct measurement of an edge particle pinch is available to date, although 2D simulations have provided indirect evidence for the need of a pinch term to explain the density profile (e.g. in the ELM-free period of a DIII-D discharge[5]). It is

speculated in [6, 7] that edge kinetic ballooning modes excited during the build-up of the pedestal pressure are responsible for the saturation of the maximum pressure gradient well before the ELM occurs. Detailed fluctuation measurements localized in the pedestal region as well as gyrokinetic simulations of small scale edge instabilities are necessary in order to support or disprove this hypothesis. In this regard, a few kinds of quasi-coherent modes have been found to be relevant with pedestal dynamics recently [8-13]. For example, DIII-D results point out that a quasi-coherent mode (kinetic ballooning mode) in the high pressure and high density pedestal region plays a critical role in sustaining the high confinement [8]. The observation on C-Mod indicates that instabilities at the edge transport barrier limit the pedestal growth [9]. The finding in EAST experiment demonstrates that the particle outflow driven by an edge coherent mode (ECM) plays a significant role in sustaining the long pulse H-mode discharges [10]. All these results indicate that the modes observed induce out going particle or energy flow to limit further development of pressure gradient in the pedestal and avoid major explosive MHD activities and confinement degradation. Nevertheless, direct experimental investigation of the dynamic evolutions of plasma parameters, including density, temperature and their gradients, in the pedestal, prior to ELM onset and in the recovering phase after its eruption, is still a lack. In addition, the roles played by the density gradient and temperature gradient may have to be distinguished. Here, we report a new quasi coherent mode (QCM) which was observed just prior to each ELM onset in H-mode plasmas on HL-2A tokamak. The mode induces an inward particle flux which contributes significant additional density and its gradient/pressure gradient increase and seems to play a major role in triggering the ELM onset. The characteristics of the mode are investigated in detail and interaction of the mode with ambient turbulence is revealed. Decoupling of particle transport from energy transport, similar to that observed in I-mode discharges [14], was observed and the dominant role of density gradient over temperature gradient for triggering ELM onset is demonstrated.

2. Experiment Setup

The high confinement mode experiment was performed deuterium plasmas on HL-2A tokamak with lower single-null divertor configurations and following parameters: $B_t = 1.4$ T, $I_p = 160$ kA, $n_{e1} = (2.0-2.5) \times 10^{19} \text{ m}^{-3}$ and $P_{\text{NBI}} = 1.0$ MW. A three-step Langmuir probe array with the diameter of 2.0 mm, length of 2.5 mm, step height of 3.0 mm are used to measure the radial distributions of local floating potential, electron temperature and density fluctuations [15]. In addition, an arc shaped or a fork probe array of 12 tips is used to measure the poloidal distributions of the fluctuations as shown in Figure 1 [16]. The innermost radial position of the probe is at $\Delta r = -15.0$ mm, where Δr is the radial displacement of the probe away from the separatrix, and the negative sign means inward from the separatrix. The sampling rate of the probes is 1 MHz, corresponding to a Nyquist frequency of 500 kHz. The results presented in this work are well reproducible whenever the probe system is input into plasmas which have ELMy H-mode confinement.

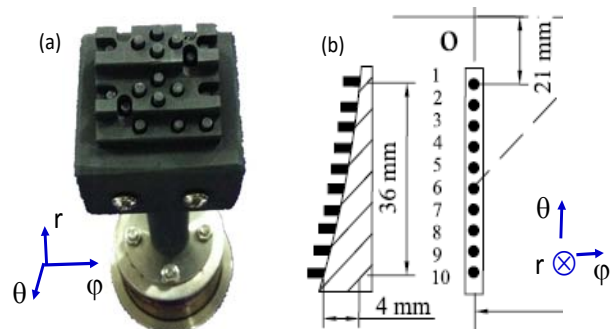


FIG. 1. The three-step Langmuir probe array (a), and the arc shaped probe array of 12 tips (b).

3. Experimental Results

3.1. Basic Characteristics of the Quasi-Coherent Mode

The quasi-coherent mode was observed in quite a few plasma parameters, such as floating potential, density and temperature fluctuations, radial electric field etc.. Given in Figure 2 are the time evolutions of ion saturation current (electron density) and floating potential fluctuations (a)-(b), their frequency spectra (c)-(d), and the poloidal propagation of floating potentials (e) in an inter-ELM phase. It is clearly shown that quasi-coherent mode exists in the floating potential and density fluctuations. The mode has a center frequency $f=60$ kHz with the half width $\Delta f=20$ kHz. A higher harmonic of frequency ~ 120 kHz appears in the density fluctuation, but not in the floating potential. The poloidal mode number and propagation velocity, which is in the electron diamagnetic drift direction in the laboratory frame, were estimated as $m \approx 20-24$ and $6.3-7.5$ km/s, respectively, using the arc-shaped 12 poloidal probe array located at $\Delta r = -10.0$ mm. From the radial probes it was estimated that the mode propagates inward with $300-400$ m/s. The toroidal mode number was estimated to be $n = m/q \approx 7-8$, using safety factor $q \approx 3$ at the edge transport barrier. The mode propagates in the direction parallel to plasma current. The amplitude of the mode peaks at about $\Delta r = -20.0$ mm. During this phase, the plasma horizontal displacement is less than 2.0 mm.

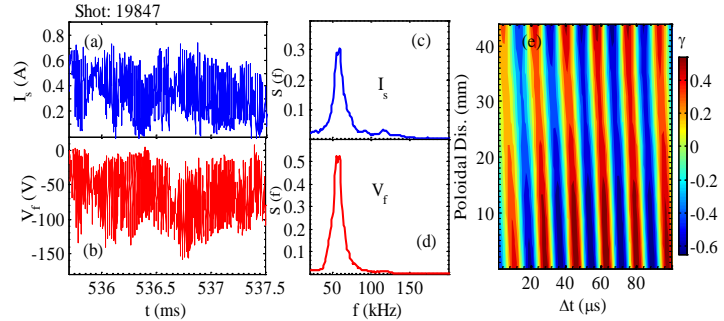


FIG. 2. The time evolutions of electron density and floating potential fluctuations (a)-(b), their frequency spectra (c)-(d), and the poloidal propagation of the floating potential (e) in an inter-ELM phase.

3.2. Non-linear Interaction Between QCM and Turbulence

The nonlinear interaction between the quasi-coherent mode and the ambient turbulence is investigated with the squared auto-bicoherence analysis, an indicator for the strength of nonlinear three-wave coupling, [17], defined as $\hat{b}^2(f = f_1 + f_2) = |B(f)|^2 / \langle |\phi(f_1)\phi(f_2)|^2 \rangle \langle |\phi(f = f_1 + f_2)|^2 \rangle$. Here, $B(f) = \langle \phi(f_1)\phi(f_2)\phi^*(f = f_1 + f_2) \rangle$ is the auto-bicoherence spectrum while $\langle \dots \rangle$ denotes an ensemble average. The probe is located in edge transport barrier ($\Delta r = -15$ mm) and the averaged

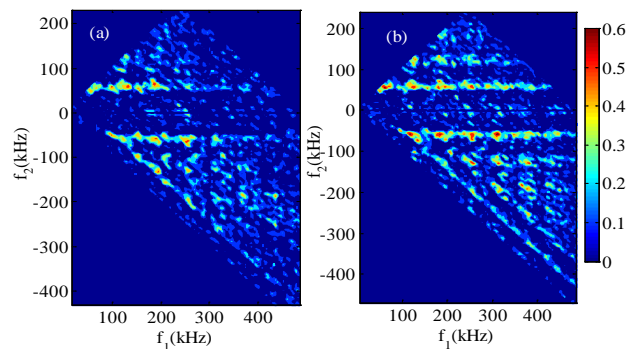


FIG. 3. The squared auto-bicoherence plot of floating potential (a) and density (b) fluctuations.

data length is about 5.0 ms. Figure 3 shows the squared auto-bicoherence $\hat{b}^2(f = f_1 + f_2)$ of the floating potential (a) and density fluctuations (b) in inter-ELMs, respectively. The squared auto-bicoherence is plotted in the region between the lines of the $f_1 - f_2 = 0$ and $f_1 + f_2 = 0$ in the $f_1 - f_2$ plane. The figure is symmetric with respect to the line $f_1 - f_2 = 0$ ($f_2 > 0$) and the line $f_1 + f_2 = 0$ ($f_2 < 0$). The intensity of the normalized bicoherence is expressed with different colors. As is

clearly shown in figure 3, that the values of $\hat{b}^2(f = f_1 + f_2)$ at $f = f_1 + f_2 = 60$ kHz and $f_2 = \pm 60$ kHz are higher than those at other frequencies. The significant nonlinear coupling is detected at two frequency ranges of $f = 60$ kHz and 120 kHz in density fluctuations. These observations suggest that there are strong three-wave nonlinear coupling between the quasi coherent mode and the ambient turbulence in inter-ELM phases. The QCM may modulate, suppress or enhance the turbulence. This will be discussed again late.

3.3. Effects of the QCM on Pedestal Dynamics

The QCM has significant influences on the evolution of plasma parameters in the pedestal just prior to each ELM onset. Shown in Figures 4 (a) and (b) are the time evolutions of D_α emission and floating potential fluctuation in shot #25108. It is not difficult to find out that the amplitude of the floating potential fluctuation starts to increase about 0.2 ms prior to each ELM onset. Actually, similar correspondences exist in quite a few physics quantities such as density fluctuation, radial electric field etc. and well reproducible in discharges of ELMy H-mode. In order to show such behaviors more clearly zoomed in plots are given in the figures 4(c)-(h) around one ELM. Here, clearly shown are that the local electron density (c) and the root mean square of the QCM of $f \sim 40$ -60 kHz in the floating potential (d) both grow first gradually and then very rapidly before an ELM crash induced density decrease. The inverse of the density gradient scale length first decreases gradually and then increases very rapidly while the inverse of the electron temperature gradient decreases continually (e) in the same period of time. In addition, the inverse of pressure gradient scale length (f) decreases first and then increases in coincidence with the increases of the local density and the inverse of its gradient scale length. Figure 4(g) presents the QCM induced particle flux which is negative, meaning an inward particle pinch, in good coincidence with the increases of the density (c) and its gradient (e). The importance of the QCM induced inward particle flux in the local particle balance is investigated as follows. The time derivative of the local electron density and the divergence of the QCM induced particle flux are estimated and the results are given in Figure 4(h). The divergence is lower than but

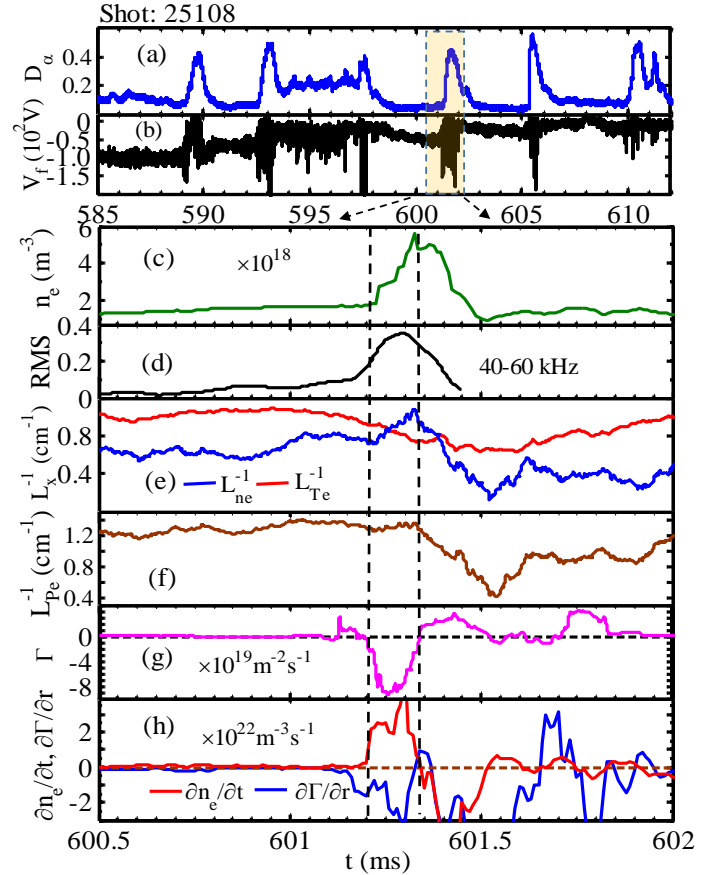


FIG. 4. Evolutions of D_α emission (a), the fluctuation of floating potential (b), the local electron density (c), the root mean square of the floating potential fluctuation of 40-60 kHz (QCM) (d), the scale lengths of the electron temperature and density gradients (e), the scale length of plasma pressure gradient (f), the particle flux induced by the QCM (g), density derivative with respect to time and the divergence of the QCM induced particle flux (h).

comparable with the time derivative. This suggests that the QCM induced particle flux makes significant contributions to the local particle balance and the observed local density increment. The particle flux given in Fig.4 (g) is calculated through the following formula,

$$\Gamma_r(f) = \frac{2}{B_\phi} k_\theta(f) |P_{n\phi}(f)| \sin[\alpha_{n\phi}(f)]$$

Given in Figure 5 are the frequency spectra of the three terms at the right hand side and the flux itself, respectively, i.e. the poloidal wave vector (a), the sinusoidal of the phase shift between the plasma potential and the density fluctuations (b), the cross power between plasma potential fluctuation and density fluctuation (c), and the particle flux (d). Here, the negative sign in Fig.5 (a) means electron diamagnetic drift direction. The QCM and the ambient turbulence are both propagate in the electron diamagnetic drift direction in the laboratory frame. A linear dispersion relation for the turbulence of $f \sim 80\text{-}130$ kHz is clearly demonstrated while it is shifted somehow in the QCM frequency region of 40-80 kHz. The phase shift between the plasma potential fluctuation and density fluctuation is approximately a constant $\pi/4$. The cross power and particle flux are concentrated in the QCM frequency region. This observation unambiguously demonstrates that the inward particle flux is mainly induced by the QCM.

The causality between the QCM fluctuation and the density gradient increase is one of the key segments in the investigation. Figure 6 gives the statistic results on the phase relation (a) and the Lissajous diagram (b) between the floating potential fluctuations and the density gradient oscillation averaged over 20 cycles just prior to ELM onsets. Figure 6(a) clearly indicates that the floating potential leads the density gradient about $\pi/4$, confirming the role of the mode in the increases of the local density and its gradient as discussed in Figure 4. The Lissajous diagram also indicates the causality between the QCM fluctuation and the density gradient, similar to the argument presented in Ref.15. It is worth pointing out that the instantaneous density gradient oscillatorily increases with time as shown in Fig.4(e) while the conditional averaged values over 20 cycles are presented here only.

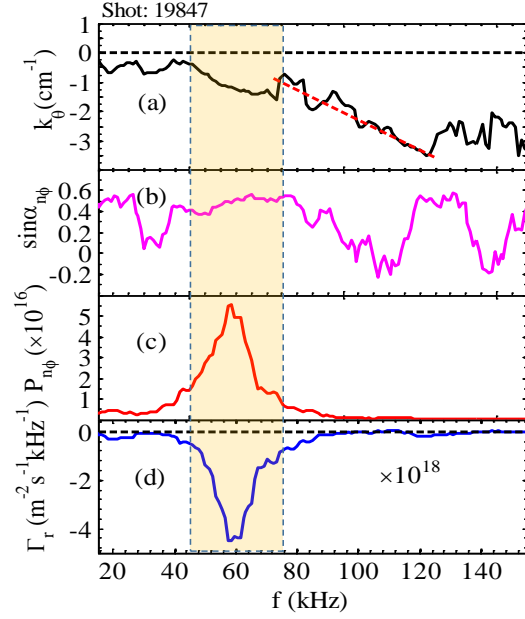


FIG. 5. The frequency spectrum of poloidal wave vector (a), the sinusoidal of the phase shift between plasma potential fluctuation and density fluctuation (b), the cross power between plasma potential fluctuation and density fluctuation (c), the particle flux (d).

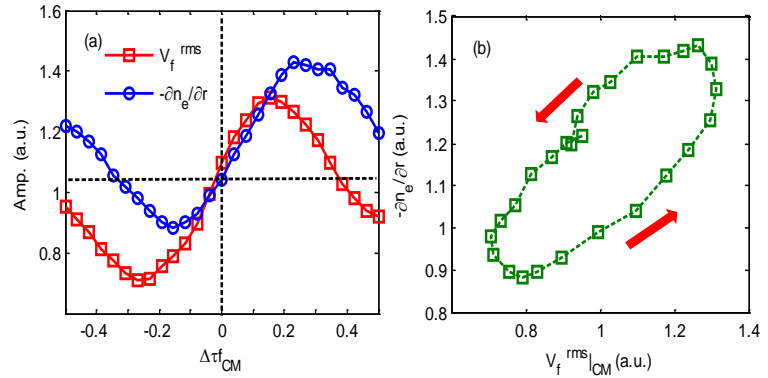


FIG. 6. The statistic results on the phase relation between the floating potential fluctuations of and the density gradient oscillation (a) and the Lissajous diagram between the floating potential fluctuations and the density gradient oscillation averaged over 20 cycles.

The role of the heat flux induced by the QCM is found to be very small in the energy balance. Shown in Figure 7 are time evolutions of the Da emission (a), the local electron temperature T_e (b), its time derivative (c) and the divergence of the local heat flux induced by the QCM (d). T_e first increases slightly and then decreases prior to the ELM onset at about $t=601.35$ ms. The time derivative of T_e close to the ELM onset is negative, in significant contrast with the density gradient. The divergence of the QCM induced heat flux is much lower than T_e time derivative. This observation clearly indicates that the QCM has slight contribution in the local energy balance and, therefore, small effect on the energy transport. On the other hand, considering that the electron temperature gradient also decreases during the existence of the QCM, we may conclude that the particle transport and energy transport induced by the QCM are completely decoupled as seen in the edge of an I-mode discharge where an edge transport barrier is observed in temperature but not in density. Here, it is the opposite that the density gradient is enhanced by the QCM while temperature gradient is reduced.

3.4. Change of Line Averaged Density and Total Particle Number

It is worth a while to point out that the QCM induced inward particle flux influences not only the local density and its gradient as shown in Figure 4 but also the line average density which also increases during the existence of the QCM. One example is given in Figure 8 where the fluctuation of the QCM floating potential (a), the QCM induced particle flux (b), and the line averaged electron density (c) are presented. The estimation of the increase of total particle number in $\Delta t = 0.15$ ms from the line averaged density increase $\Delta n_{e\perp} = 0.01 \times 10^{19} \text{ m}^{-3}$ is $\Delta N_e = \Delta n_{e\perp} V \approx 9.5 \times 10^{17}$ with V being the volume of the plasma column. The contribution from the QCM induced inward particle flux is $\Delta N_{e_m} = \Gamma dt S_0 = 8.5 \times 10^{19} \times 1.5 \times 10^{-4} \times 23.8 = 3.0 \times 10^{17}$ with dt and S_0 being the QCM existing time length and the area of the plasma surface, respectively. The QCM induced inward particle flux makes approximately one third of the total particle increment.

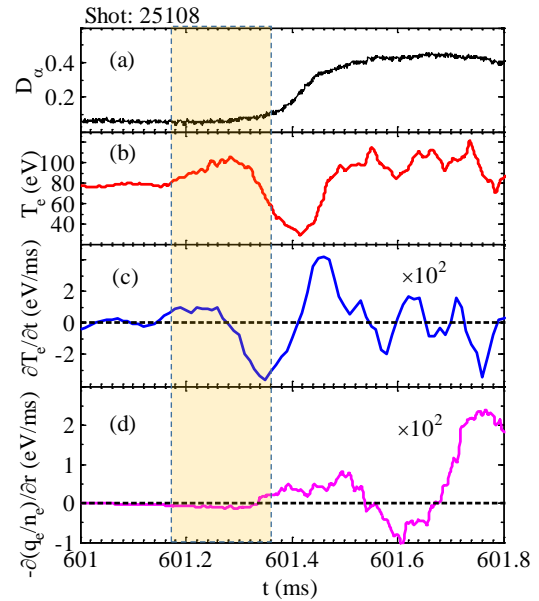


FIG. 7. The evolutions of Da emission (a), the electron temperature (b), the time derivative of electron temperature (c), the divergence of heat flux induced by the QCM (d).

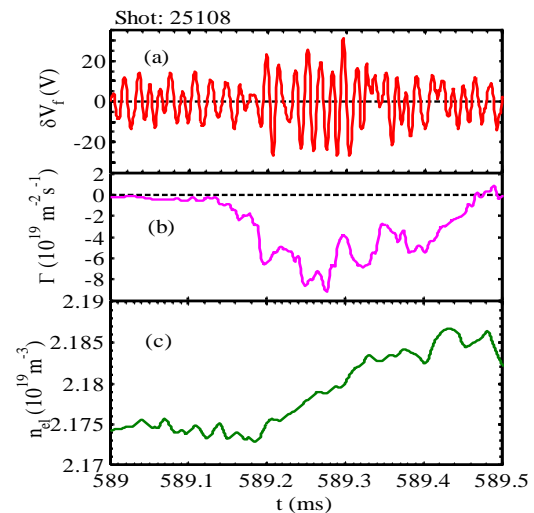


FIG. 8. The evolutions of QCM in floating potential (a), the QCM induced particle flux (b), and the line averaged electron density (c).

3.5. Particle Loss Detected at Divertor Plate

The effect of the QCM induced inward particle flux was also observed on the divertor plates. Given in Figure 9 are the time evolutions of D_α emission (a), the particle flux detected by the divertor probe at a strike point (b), and the zoomed in plots of particle flux (c), the floating potential fluctuation of QCM (d), and the oscillating parts of the particle flux and QCM (e). Generally speaking, the particle flux is highly coincident with ELM oscillation as expected. In addition, the particle flux is modulated by the QCM oscillation as shown in Figs.9(c) and (d). Furthermore, the phase shift between the particle flux and the floating potential of the QCM evolves and becomes completely out of phase just prior to the ELM onset as shown in Fig.9 (e). This is an explicit evidence revealing that the QCM induces inward particle flux in the pedestal and reduces particle loss from the edge plasma to the divertor.

It is important to point out that the results presented above are very similar prior to each ELM onset.

4. Concluding Summary and Discussion

The detailed analyses of the dynamic evolutions of plasma parameters, including density, temperature, pressure and their gradients in pedestal are presented for recent H-mode experiments on HL-2A tokamak. A quasi-coherent mode of a center frequency $f \sim 40\text{--}60$ kHz with the half width $\Delta f = 20$ kHz was observed just prior to each ELM onset in a series. The mode was observed in floating potential, density and its gradient, electron temperature and its gradient, radial electric field etc. and grows very rapidly just about 200 microseconds before each ELM onset. The characteristics of the mode are identified. The mode propagates in electron diamagnetic drift direction poloidally, parallel to plasma current toroidally and inward radially. The auto-power spectrum analysis indicates that the mode frequency peaks at $f = 40\text{--}60$ kHz. The poloidal and toroidal wave vectors are $m \sim 20\text{--}24$ and $n \sim 7\text{--}8$, respectively. The mode peaks at about $\Delta r = -20.0$ mm radially. The squared auto-bicoherence analyses of the floating potential and density fluctuations indicate that the mode has strong nonlinear interaction with the ambient turbulence. The mode induces an inward particle flux and an outward heat flux. The mode induced fluxes lead to the dramatic increase of density and its gradient, and slight decrease of electron temperature and its gradient just prior to each ELM onset observed in the experiment. The inward particle flux plays a dominant role in the particle balance and increases of density and its gradient in the pedestal before each ELM onset. The mode also induces increases of plasma pressure and its gradient and may play a key role in triggering of ELM onset.

On the other hand, the role of the mode induced outward heat flux is small and almost

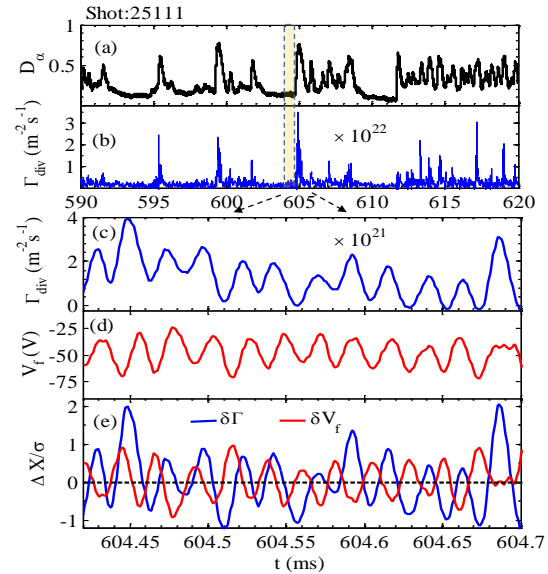


FIG. 9. Evolutions of D_α emission (a), the particle flux received by the divertor probes at strike point (b), and the zoomed in plots of particle flux (c), the floating potential fluctuation of QCM (d), the oscillating parts of the particle flux and the QCM (e).

negligible in the energy balance in the pedestal. These observations indicate that the QCM induced energy transport is decoupled from the density diffusion, resembling the observations in I-mode discharges where there are L-mode density profiles and H-mode temperature profiles in the pedestals, simultaneously. In addition, it is observed that the gradient scale length of the electron density is always shorter than that of the electron temperature at the starting point of the ELM onset and, therefore, possible dominant role of density gradient over temperature gradient for ELM inducing is demonstrated. The results are consistent with I-mode discharges where high temperature gradient does not lead to ELM onset. Finally, the QCM presented in this work is in significant contrast with the previously reported quasi-coherent modes which induce outward particle or heat flux and help sustaining H-mode discharges.

Acknowledgements

This work is supported by the National Magnetic Confinement Fusion Science Program No. 2013GB112008, No. 2014GB108000, No. 2014GB107000, and No. 2013GB107001; by the National Natural Science Foundation of China, No. 11375054, No. 11175060, No. 91130031, No. 10990213, and No. 11320101005; by Grant-in-Aid for Scientific Research of JSPS (15H02155, 15H02335, and 16H02442).

References:

- [1] WAGNER, F., *et al.*, 1982 *Phys. Rev. Lett.* [49 1408](#)
- [2] SNYDER, P. B., *et al.*, 2002 *Phys. Plasmas* **9** 2037
- [3] DOYLE, E.J., *et al.*, 2007 *Nucl. Fusion* **47** S18
- [4] LOARTE, A., *et al.*, 2003 *Plasma Phys. Control. Fusion* **45** 1549
- [5] STACEY, W. M., *et al.*, 2009 *Phys. of Plasmas* **16**, 102504
- [6] WILSON, H. R., *et al.*, 2006 *Plasma Phys. Controlled Fusion* **48** A71
- [7] SNYDER, P.B., *et al.*, 2011 *Nucl. Fusion* **51** 103016
- [8] YAN, Z., *et al.*, 2011 *Phys. Rev. Lett.* [107 055004](#)
- [9] MAZURENKO, A., *et al.*, 2002 *Phys. Rev. Lett.* **89** 225004
- [10] DIALLO, A., *et al.*, 2014 *Phys. Rev. Lett.* [112 115001](#)
- [11] WANG, H.Q., *et al.*, 2014 *Phys. Rev. Lett.* [112 185004](#)
- [12] GAO, X., *et al.*, 2015 *Nuclear Fusion* **55** 083015
- [13] ZHONG, W.L., *et al.*, 2016 *Plasma Phys. Control. Fusion* **58** 065001
- [14] HUBBARD, E., *et al.*, 2016 *Nuclear Fusion* **56** 086003
- [15] CHENG, J., *et al.*, 2013 *Phys. Rev. Lett.* [110 265002](#)
- [16] CHENG, J., *et al.*, 2013 *Nucl. Fusion* **53** 093008
- [17] KIM, Y.C. and POWERS E.J., 1979 *IEEE Trans. Plasma Sci.* [PS-7 120](#)